Search for Radiative Penguin Decays $B^+ \to \rho^+\gamma$, $B^0 \to \rho^0\gamma$, and $B^0 \to \omega\gamma$

B. Aubert,[1] R. Barate,[1] D. Boutigny,[1] F. Couderc,[1] J.-M. Gaillard,[1] A. Hicheur,[1] Y. Karyotakis,[1] J. P. Lees,[1] V. Tisserand,[1] A. Zghiche,[1] A. Palano,[2] A. Pompili,[2] J. C. Chen,[3] N. D. Qi,[3] G. Rong,[3] P. Wang,[3] Y. S. Zhu,[3] G. Eigen,[4] I. Ofte,[4] B. Stugu,[4] G. S. Abrams,[5] A. W. Borgland,[5] A. B. Breon,[5] D. N. Brown,[5] J. Button-Shafer,[5] R. N. Cahn,[5] E. Charles,[5] C. T. Day,[5] M. S. Gill,[5] A. V. Gritsan,[5] Y. Groysman,[5] R. G. Jacobsen,[5] R. W. Kadel,[5] J. Kadyk,[5] L. T. Kerth,[5] Yu. G. Kolomensky,[5] G. Kukartsev,[5] G. Lynch,[5] L. M. Mir,[5] P. J. Oddone,[5] T. J. Orimoto,[5] M. Pripstein,[5] N. A. Roe,[5] M. T. Ronan,[5] V. G. Shelkov,[5] W. A. Wenzel,[5] M. Barrett,[6] K. E. Ford,[6] T. J. Harrison,[6] A. J. Hart,[6] C. M. Hawkes,[6] S. E. Morgan,[6] A. T. Watson,[6] M. Fritsch,[7] K. Goetzen,[7] T. Held,[7] H. Koch,[7] B. Lewandowski,[7] M. Pelizaeus,[7] M. Steinke,[7] J. T. Boyd,[8] N. Chevalier,[8] W. N. Cottingham,[8] M. P. Kelly,[8] T. E. Latham,[8] F. F. Wilson,[8] T. Cuhadar-Donszelmann,[9] C. Hearty,[9] N. S. Knecht,[9] T. S. Mattison,[9] J. A. McKenna,[9] D. Thiessen,[9] A. Khan,[10] P. Kyberd,[10] L. Teodorescu,[10] A. E. Blinov,[11] V. E. Blinov,[11] V. P. Druzhinin,[11] V. B. Golubev,[11] V. N. Ivanchenko,[11] E. A. Kravchenko,[11] A. P. Onuchin,[11] S. I. Serednyakov,[11] Yu. I. Skovpen,[11] E. P. Solodov,[11] A. N. Yushkov,[11] D. Best,[12] M. Bruinsma,[12] M. Chao,[12] I. Eschrich,[12] D. Kirkby,[12] A. J. Lankford,[12] M. Mandelkern,[12] R. K. Mommsen,[12] W. Roethel,[12] D. P. Stoker,[12] C. Buchanan,[13] B. L. Hartfiel,[13] S. D. Foulkes,[14] J. W. Gary,[14] B. C. Shen,[14] K. Wang,[14] D. del Re,[15] H. K. Hadavand,[15] E. J. Hill,[15] D. B. MacFarlane,[15] H. P. Paar,[15] Sh. Rahatlou,[15] V. Sharma,[15] J. W. Berryhill,[16] C. Campagnari,[16] B. Dahmes,[16] O. Long,[16] A. Lu,[16] M. A. Mazur,[16] J. D. Richman,[16] W. Verkerke,[16] T. W. Beck,[17] A. M. Eisner,[17] C. A. Heusch,[17] J. Kroseberg,[17] W. S. Lockman,[17] G. Nesom,[17] T. Schalk,[17] B. A. Schumm,[17] A. Seiden,[17] P. Spradlin,[17] D. C. Williams,[17] M. G. Wilson,[17] J. Albert,[18] E. Chen,[18] G. P. Dubois-Felsmann,[18] A. Dvoretskii,[18] D. G. Hitlin,[18] I. Narsky,[18] T. Piatenko,[18] F. C. Porter,[18] A. Ryd,[18] A. Samuel,[18] S. Yang,[18] S. Jayatilleke,[19] G. Mancinelli,[19] B. T. Meadows,[19] M. D. Sokoloff,[19] T. Abe,[20] F. Blanc,[20] P. Bloom,[20] S. Chen,[20] W. T. Ford,[20] U. Nauenberg,[20] A. Olivas,[20] P. Rankin,[20] J. G. Smith,[20] J. Zhang,[20] L. Zhang,[20] A. Chen,[21] J. L. Harton,[21] A. Soffer,[21] W. H. Toki,[21] R. J. Wilson,[21] Q. L. Zeng,[21] D. Altenburg,[22] T. Brandt,[22] J. Brose,[22] M. Dickopp,[22] E. Feltresi,[22] A. Hauke,[22] H. M. Lacker,[22] R. Müller-Pfefferkorn,[22] R. Nogowski,[22] S. Otto,[22] A. Petzold,[22] J. Schubert,[22] K. R. Schubert,[22] R. Schwierz,[22] B. Spaan,[22] J. E. Sundermann,[22] D. Bernard,[23] G. R. Bonneaud,[23] F. Brochard,[23] P. Grenier,[23] S. Schrenk,[23] Ch. Thiebaux,[23] G. Vasileiadis,[23] M. Verderi,[23] D. J. Bard,[24] P. J. Clark,[24] D. Lavin,[24] F. Muheim,[24] S. Playfer,[24] Y. Xie,[24] M. Andreotti,[25] V. Azzolini,[25] D. Bettoni,[25] C. Bozzi,[25] R. Calabrese,[25] G. Cibinetto,[25] E. Luppi,[25] M. Negrini,[25] L. Piemontese,[25] A. Sarti,[25] E. Treadwell,[26] F. Anulli,[27] R. Baldini-Ferroli,[27] A. Calcaterra,[27] R. de Sangro,[27] G. Finocchiaro,[27] P. Patteri,[27] I. M. Peruzzi,[27] M. Piccolo,[27] A. Zallo,[27] A. Buzzo,[28] R. Capra,[28] R. Contri,[28] G. Crosetti,[28] M. Lo Vetere,[28] M. Macri,[28] M. R. Monge,[28] S. Passaggio,[28] C. Patrignani,[28] E. Robutti,[28] A. Santroni,[28] S. Tosi,[28] S. Bailey,[29] G. Brandenburg,[29] K. S. Chaisanguanthum,[29] M. Morii,[29] E. Won,[29] R. S. Dubitzky,[30] U. Langenegger,[30] W. Bhimji,[31] D. A. Bowerman,[31] P. D. Dauncey,[31] U. Egede,[31] J. R. Gaillard,[31] G. W. Morton,[31] J. A. Nash,[31] M. B. Nikolich,[31] G. P. Taylor,[31] M. J. Charles,[32] G. J. Grenier,[32] U. Mallik,[32] J. Cochran,[33] H. B. Crawley,[33] J. Lamsa,[33] W. T. Meyer,[33] S. Prell,[33] E. I. Rosenberg,[33] A. E. Rubin,[33] J. Yi,[33] M. Biasini,[34] R. Covarelli,[34] M. Pioppi,[34] M. Davier,[35] X. Giroux,[35] G. Grosdidier,[35] A. Höcker,[35] S. Laplace,[35] F. Le Diberder,[35] V. Lepeltier,[35] A. M. Lutz,[35] T. C. Petersen,[35] S. Plaszczynski,[35] M. H. Schune,[35] L. Tantot,[35] G. Wormser,[35] C. H. Cheng,[36] D. J. Lange,[36] M. C. Simani,[36] D. M. Wright,[36] A. J. Bevan,[37] C. A. Chavez,[37] J. P. Coleman,[37] I. J. Forster,[37] J. R. Fry,[37] E. Gabathuler,[37] R. Gamet,[37] D. E. Hutchcroft,[37] R. J. Parry,[37] D. J. Payne,[37] R. J. Sloane,[37] C. Touramanis,[37] J. J. Back,[38,*] C. M. Cormack,[38] P. F. Harrison,[38,*] F. Di Lodovico,[38] G. B. Mohanty,[38,*] C. L. Brown,[39] G. Cowan,[39] R. L. Flack,[39] H. U. Flaecher,[39] M. G. Green,[39] P. S. Jackson,[39] T. R. McMahon,[39] S. Ricciardi,[39] F. Salvatore,[39] M. A. Winter,[39] D. Brown,[40] C. L. Davis,[40] J. Allison,[41] N. R. Barlow,[41] R. J. Barlow,[41] P. A. Hart,[41] M. C. Hodgkinson,[41] G. D. Lafferty,[41] A. J. Lyon,[41] J. C. Williams,[41] A. Farbin,[42] W. D. Hulsbergen,[42] A. Jawahery,[42] D. Kovalskyi,[42] C. K. Lae,[42] V. Lillard,[42] D. A. Roberts,[42] G. Blaylock,[43] C. Dallapiccola,[43] K. T. Flood,[43] S. S. Hertzbach,[43] R. Kofler,[43] V. B. Koptchev,[43] T. B. Moore,[43] S. Saremi,[43] H. Staengle,[43] S. Willocq,[43] R. Cowan,[44] G. Sciolla,[44] S. J. Sekula,[44] F. Taylor,[44] R. K. Yamamoto,[44] D. J. J. Mangeol,[45] P. M. Patel,[45] S. H. Robertson,[45] A. Lazzaro,[46] V. Lombardo,[46] F. Palombo,[46] J. M. Bauer,[47] L. Cremaldi,[47] V. Eschenburg,[47] R. Godang,[47] R. Kroeger,[47] J. Reidy,[47] D. A. Sanders,[47] D. J. Summers,[47] H. W. Zhao,[47] S. Brunet,[48] D. Côté,[48] P. Taras,[48] H. Nicholson,[49] N. Cavallo,[50,†] F. Fabozzi,[50,†] C. Gatto,[50] L. Lista,[50] D. Monorchio,[50] P. Paolucci,[50] D. Piccolo,[50] C. Sciacca,[50] M. Baak,[51] H. Bulten,[51] G. Raven,[51] H. L. Snoek,[51] L. Wilden,[51] C. P. Jessop,[52] J. M. LoSecco,[52] T. Allmendinger,[53] K. K. Gan,[53] K. Honscheid,[53] D. Hufnagel,[53] H. Kagan,[53] R. Kass,[53] T. Pulliam,[53] A. M. Rahimi,[53] R. Ter-Antonyan,[53] Q. K. Wong,[53] J. Brau,[54] R. Frey,[54] O. Igonkina,[54] C. T. Potter,[54]

N. B. Sinev,[54] D. Strom,[54] E. Torrence,[54] F. Colecchia,[55] A. Dorigo,[55] F. Galeazzi,[55] M. Margoni,[55] M. Morandin,[55] M. Posocco,[55] M. Rotondo,[55] F. Simonetto,[55] R. Stroili,[55] G. Tiozzo,[55] C. Voci,[55] M. Benayoun,[56] H. Briand,[56] J. Chauveau,[56] P. David,[56] Ch. de la Vaissière,[56] L. Del Buono,[56] O. Hamon,[56] M. J. J. John,[56] Ph. Leruste,[56] J. Malcles,[56] J. Ocariz,[56] M. Pivk,[56] L. Roos,[56] S. T'Jampens,[56] G. Therin,[56] P. F. Manfredi,[57] V. Re,[57] P. K. Behera,[58] L. Gladney,[58] Q. H. Guo,[58] J. Panetta,[58] C. Angelini,[59] G. Batignani,[59] S. Bettarini,[59] M. Bondioli,[59] F. Bucci,[59] G. Calderini,[59] M. Carpinelli,[59] F. Forti,[59] M. A. Giorgi,[59] A. Lusiani,[59] G. Marchiori,[59] F. Martinez-Vidal,[59,‡] M. Morganti,[59] N. Neri,[59] E. Paoloni,[59] M. Rama,[59] G. Rizzo,[59] F. Sandrelli,[59] J. Walsh,[59] M. Haire,[60] D. Judd,[60] K. Paick,[60] D. E. Wagoner,[60] N. Danielson,[61] P. Elmer,[61] Y. P. Lau,[61] C. Lu,[61] V. Miftakov,[61] J. Olsen,[61] A. J. S. Smith,[61] A. V. Telnov,[61] F. Bellini,[62] G. Cavoto,[61,62] R. Faccini,[62] F. Ferrarotto,[62] F. Ferroni,[62] M. Gaspero,[62] L. Li Gioi,[62] M. A. Mazzoni,[62] S. Morganti,[62] M. Pierini,[62] G. Piredda,[62] F. Safai Tehrani,[62] C. Voena,[62] S. Christ,[63] G. Wagner,[63] R. Waldi,[63] T. Adye,[64] N. De Groot,[64] B. Franek,[64] N. I. Geddes,[64] G. P. Gopal,[64] E. O. Olaiya,[64] R. Aleksan,[65] S. Emery,[65] A. Gaidot,[65] S. F. Ganzhur,[65] P.-F. Giraud,[65] G. Hamel de Monchenault,[65] W. Kozanecki,[65] M. Legendre,[65] G. W. London,[65] B. Mayer,[65] G. Schott,[65] G. Vasseur,[65] Ch. Yèche,[65] M. Zito,[65] M. V. Purohit,[66] A. W. Weidemann,[66] J. R. Wilson,[66] F. X. Yumiceva,[66] D. Aston,[67] R. Bartoldus,[67] N. Berger,[67] A. M. Boyarski,[67] O. L. Buchmueller,[67] R. Claus,[67] M. R. Convery,[67] M. Cristinziani,[67] G. De Nardo,[67] D. Dong,[67] J. Dorfan,[67] D. Dujmic,[67] W. Dunwoodie,[67] E. E. Elsen,[67] S. Fan,[67] R. C. Field,[67] T. Glanzman,[67] S. J. Gowdy,[67] T. Hadig,[67] V. Halyo,[67] C. Hast,[67] T. Hryn'ova,[67] W. R. Innes,[67] M. H. Kelsey,[67] P. Kim,[67] M. L. Kocian,[67] D. W. G. S. Leith,[67] J. Libby,[67] S. Luitz,[67] V. Luth,[67] H. L. Lynch,[67] H. Marsiske,[67] R. Messner,[67] D. R. Muller,[67] C. P. O'Grady,[67] V. E. Ozcan,[67] A. Perazzo,[67] M. Perl,[67] S. Petrak,[67] B. N. Ratcliff,[67] A. Roodman,[67] A. A. Salnikov,[67] R. H. Schindler,[67] J. Schwiening,[67] G. Simi,[67] A. Snyder,[67] A. Soha,[67] J. Stelzer,[67] D. Su,[67] M. K. Sullivan,[67] J. Va'vra,[67] S. R. Wagner,[67] M. Weaver,[67] A. J. R. Weinstein,[67] W. J. Wisniewski,[67] M. Wittgen,[67] D. H. Wright,[67] A. K. Yarritu,[67] C. C. Young,[67] P. R. Burchat,[68] A. J. Edwards,[68] T. I. Meyer,[68] B. A. Petersen,[68] C. Roat,[68] S. Ahmed,[69] M. S. Alam,[69] J. A. Ernst,[69] M. A. Saeed,[69] M. Saleem,[69] F. R. Wappler,[69] W. Bugg,[70] M. Krishnamurthy,[70] S. M. Spanier,[70] R. Eckmann,[71] H. Kim,[71] J. L. Ritchie,[71] A. Satpathy,[71] R. F. Schwitters,[71] J. M. Izen,[72] I. Kitayama,[72] X. C. Lou,[72] S. Ye,[72] F. Bianchi,[73] M. Bona,[73] F. Gallo,[73] D. Gamba,[73] L. Bosisio,[74] C. Cartaro,[74] F. Cossutti,[74] G. Della Ricca,[74] S. Dittongo,[74] S. Grancagnolo,[74] L. Lanceri,[74] P. Poropat,[74,§] L. Vitale,[74] G. Vuagnin,[74] R. S. Panvini,[75] Sw. Banerjee,[76] C. M. Brown,[76] D. Fortin,[76] P. D. Jackson,[76] R. Kowalewski,[76] J. M. Roney,[76] R. J. Sobie,[76] H. R. Band,[77] B. Cheng,[77] S. Dasu,[77] M. Datta,[77] A. M. Eichenbaum,[77] M. Graham,[77] J. J. Hollar,[77] J. R. Johnson,[77] P. E. Kutter,[77] H. Li,[77] R. Liu,[77] A. Mihalyi,[77] A. K. Mohapatra,[77] Y. Pan,[77] R. Prepost,[77] P. Tan,[77] J. H. von Wimmersperg-Toeller,[77] J. Wu,[77] S. L. Wu,[77] Z. Yu,[77] M. G. Greene,[78] and H. Neal[78]

(*BABAR* Collaboration)

[1]*Laboratoire de Physique des Particules, F-74941 Annecy-le-Vieux, France*
[2]*Università di Bari, Dipartimento di Fisica and INFN, I-70126 Bari, Italy*
[3]*Institute of High Energy Physics, Beijing 100039, China*
[4]*University of Bergen, Institute of Physics, N-5007 Bergen, Norway*
[5]*Lawrence Berkeley National Laboratory and University of California, Berkeley, California 94720, USA*
[6]*University of Birmingham, Birmingham, B15 2TT, United Kingdom*
[7]*Ruhr Universität Bochum, Institut für Experimentalphysik 1, D-44780 Bochum, Germany*
[8]*University of Bristol, Bristol BS8 1TL, United Kingdom*
[9]*University of British Columbia, Vancouver, British Columbia V6T 1Z1, Canada*
[10]*Brunel University, Uxbridge, Middlesex UB8 3PH, United Kingdom*
[11]*Budker Institute of Nuclear Physics, Novosibirsk 630090, Russia*
[12]*University of California at Irvine, Irvine, California 92697, USA*
[13]*University of California at Los Angeles, Los Angeles, California 90024, USA*
[14]*University of California at Riverside, Riverside, California 92521, USA*
[15]*University of California at San Diego, La Jolla, California 92093, USA*
[16]*University of California at Santa Barbara, Santa Barbara, California 93106, USA*
[17]*University of California at Santa Cruz, Santa Cruz, California 95064, USA*
[18]*California Institute of Technology, Pasadena, California 91125, USA*
[19]*University of Cincinnati, Cincinnati, Ohio 45221, USA*
[20]*University of Colorado, Boulder, Colorado 80309, USA*
[21]*Colorado State University, Fort Collins, Colorado 80523, USA*
[22]*Technische Universität Dresden, Institut für Kern- und Teilchenphysik, D-01062 Dresden, Germany*
[23]*Ecole Polytechnique, LLR, F-91128 Palaiseau, France*

[24]University of Edinburgh, Edinburgh EH9 3JZ, United Kingdom
[25]Università di Ferrara, Dipartimento di Fisica and INFN, I-44100 Ferrara, Italy
[26]Florida A&M University, Tallahassee, Florida 32307, USA
[27]Laboratori Nazionali di Frascati dell'INFN, I-00044 Frascati, Italy
[28]Università di Genova, Dipartimento di Fisica and INFN, I-16146 Genova, Italy
[29]Harvard University, Cambridge, Massachusetts 02138, USA
[30]Universität Heidelberg, Physikalisches Institut, Philosophenweg 12, D-69120 Heidelberg, Germany
[31]Imperial College London, London, SW7 2AZ, United Kingdom
[32]University of Iowa, Iowa City, Iowa 52242, USA
[33]Iowa State University, Ames, Iowa 50011-3160, USA
[34]Università di Perugia, Dipartimento di Fisica and INFN, I-06100 Perugia, Italy
[35]Laboratoire de l'Accélérateur Linéaire, F-91898 Orsay, France
[36]Lawrence Livermore National Laboratory, Livermore, California 94550, USA
[37]University of Liverpool, Liverpool L69 72E, United Kingdom
[38]Queen Mary, University of London, E1 4NS, United Kingdom
[39]University of London, Royal Holloway and Bedford New College, Egham, Surrey TW20 0EX, United Kingdom
[40]University of Louisville, Louisville, Kentucky 40292, USA
[41]University of Manchester, Manchester M13 9PL, United Kingdom
[42]University of Maryland, College Park, Maryland 20742, USA
[43]University of Massachusetts, Amherst, Massachusetts 01003, USA
[44]Massachusetts Institute of Technology, Laboratory for Nuclear Science, Cambridge, Massachusetts 02139, USA
[45]McGill University, Montréal, Quebec H3A 2T8, Canada
[46]Università di Milano, Dipartimento di Fisica and INFN, I-20133 Milano, Italy
[47]University of Mississippi, University, Mississippi 38677, USA
[48]Université de Montréal, Laboratoire René J. A. Lévesque, Montréal, Quebec H3C 3J7 Canada
[49]Mount Holyoke College, South Hadley, Massachusetts 01075, USA
[50]Università di Napoli Federico II, Dipartimento di Scienze Fisiche and INFN, I-80126, Napoli, Italy
[51]NIKHEF, National Institute for Nuclear Physics and High Energy Physics, NL-1009 DB Amsterdam, The Netherlands
[52]University of Notre Dame, Notre Dame, Indiana 46556, USA
[53]Ohio State University, Columbus, Ohio 43210, USA
[54]University of Oregon, Eugene, Oregon 97403, USA
[55]Università di Padova, Dipartimento di Fisica and INFN, I-35131 Padova, Italy
[56]Universités Paris VI et VII, Laboratoire de Physique Nucléaire et de Hautes Energies, F-75252 Paris, France
[57]Università di Pavia, Dipartimento di Elettronica and INFN, I-27100 Pavia, Italy
[58]University of Pennsylvania, Philadelphia, Pennsylvania 19104, USA
[59]Università di Pisa, Dipartimento di Fisica, Scuola Normale Superiore and INFN, I-56127 Pisa, Italy
[60]Prairie View A&M University, Prairie View, Texas 77446, USA
[61]Princeton University, Princeton, New Jersey 08544, USA
[62]Università di Roma La Sapienza, Dipartimento di Fisica and INFN, I-00185 Roma, Italy
[63]Universität Rostock, D-18051 Rostock, Germany
[64]Rutherford Appleton Laboratory, Chilton, Didcot, Oxon, OX11 0QX, United Kingdom
[65]DSM/Dapnia, CEA/Saclay, F-91191 Gif-sur-Yvette, France
[66]University of South Carolina, Columbia, South Carolina 29208, USA
[67]Stanford Linear Accelerator Center, Stanford, California 94309, USA
[68]Stanford University, Stanford, California 94305-4060, USA
[69]State University of New York, Albany, New York 12222, USA
[70]University of Tennessee, Knoxville, Tennessee 37996, USA
[71]University of Texas at Austin, Austin, Texas 78712, USA
[72]University of Texas at Dallas, Richardson, Texas 75083, USA
[73]Università di Torino, Dipartimento di Fisica Sperimentale and INFN, I-10125 Torino, Italy
[74]Università di Trieste, Dipartimento di Fisica and INFN, I-34127 Trieste, Italy
[75]Vanderbilt University, Nashville, Tennessee 37235, USA
[76]University of Victoria, Victoria, British Columbia V8W 3P6 Canada
[77]University of Wisconsin, USA, Madison, Wisconsin 53706, USA
[78]Yale University, New Haven, Connecticut 06511, USA
(Received 11 August 2004; published 3 January 2005)

A search for the decays $B \to \rho(770)\gamma$ and $B^0 \to \omega(782)\gamma$ is performed on a sample of 211×10^6 $\Upsilon(4S) \to B\overline{B}$ events collected by the *BABAR* detector at the SLAC PEP-II asymmetric-energy e^+e^- storage ring. No evidence for the decays is seen. We set the following limits on the individual branching fractions: $\mathcal{B}(B^+ \to \rho^+\gamma) < 1.8 \times 10^{-6}$, $\mathcal{B}(B^0 \to \rho^0\gamma) < 0.4 \times 10^{-6}$, and $\mathcal{B}(B^0 \to \omega\gamma) < 1.0 \times 10^{-6}$ at

the 90% confidence level. We use the quark model to limit the combined branching fraction $\overline{\mathcal{B}}[B \to (\rho/\omega)\gamma] < 1.2 \times 10^{-6}$, from which we determine a constraint on the ratio of Cabibbo-Kobayashi-Maskawa matrix elements $|V_{td}|/|V_{ts}|$.

DOI: 10.1103/PhysRevLett.94.011801 PACS numbers: 13.20.He, 12.15.Hh

Within the standard model (SM), the decays $B \to \rho\gamma$ and $B^0 \to \omega\gamma$ proceed primarily through a $b \to d\gamma$ electromagnetic penguin process that contains a top quark within the loop [1]. The rates for $B^+ \to \rho^+\gamma$, $B^0 \to \rho^0\gamma$, and $B^0 \to \omega\gamma$ [2] are related by the spectator-quark model, and we define the average branching fraction [3], $\overline{\mathcal{B}}[B \to (\rho/\omega)\gamma] = \frac{1}{2}\{\mathcal{B}(B^+ \to \rho^+\gamma) + (\tau_{B^+}/\tau_{B^0}) \times [\mathcal{B}(B^0 \to \rho^0\gamma) + \mathcal{B}(B^0 \to \omega\gamma)]\}$, where τ_{B^+}/τ_{B^0} is the ratio of B-meson lifetimes. Recent calculations of $\overline{\mathcal{B}}[B \to (\rho/\omega)\gamma]$ in the SM indicate a range of $(0.9\text{-}1.8) \times 10^{-6}$ [3,4]. There may also be contributions resulting from physics beyond the SM [5]. The ratio between the branching fractions for $B \to (\rho/\omega)\gamma$ and $B \to K^*\gamma$ is related in the SM to the ratio of Cabibbo-Kobayashi-Maskawa (CKM) matrix elements $|V_{td}|/|V_{ts}|$ [3,6]. Previous searches by *BABAR* [7] and CLEO [8] have found no evidence for $B \to (\rho/\omega)\gamma$ decays.

We search for $B \to \rho\gamma$ and $B^0 \to \omega\gamma$ decays in a data sample containing $(211 \pm 2) \times 10^6$ $\Upsilon(4S) \to B\overline{B}$ decays, collected by the *BABAR* detector [9] at the SLAC PEP-II asymmetric-energy e^+e^- storage ring. The data correspond to an integrated luminosity of 191 fb^{-1}.

The decay $B \to \rho\gamma$ is reconstructed with $\rho^0 \to \pi^+\pi^-$ and $\rho^+ \to \pi^+\pi^0$, while $B^0 \to \omega\gamma$ is reconstructed with $\omega \to \pi^+\pi^-\pi^0$. Background comes primarily from $e^+e^- \to q\bar{q}$ continuum events, where $q = u, d, s, c$, in which a high-energy photon is produced through $\pi^0/\eta \to \gamma\gamma$ decays or via initial-state radiation (ISR). There are also significant $B\overline{B}$ backgrounds: $B \to K^*\gamma$, $K^* \to K\pi$, where a $K^\pm$ is misidentified as a $\pi^\pm$; $B \to (\rho/\omega)\pi^0$ and $B \to (\rho/\omega)\eta$, where a high-energy photon comes from the π^0 or η decay; and combinatorial background, mostly from high multiplicity $b \to s\gamma$ decays.

We select $\pi^\pm$ candidates from tracks with a momentum transverse to the beam direction greater than 100 MeV/c. The $\pi^\pm$ selection algorithm combines measurements of energy loss in the tracking system with any associated Cherenkov photons measured by the ring imaging Cherenkov detector. The algorithm is optimized to reduce backgrounds from $K^\pm$ produced in $b \to s\gamma$ processes [7].

Neutral pion candidates are identified as pairs of neutral energy-deposits reconstructed in the CsI crystal calorimeter, each with an energy greater than 50 MeV in the laboratory frame. For $B^0 \to \omega\gamma$ ($B^+ \to \rho^+\gamma$) decays, the invariant mass of the pair is required to satisfy $110 < m_{\gamma\gamma} < 150$ MeV/c^2 ($117 < m_{\gamma\gamma} < 145$ MeV/c^2). To reduce combinatorial background, we require the cosine of the opening angle between the daughter photons in the laboratory frame be greater than 0.6; this selection retains 98% of π^0 from signal decays.

A ρ^0 candidate is reconstructed by selecting two identified pions that have opposite charge and a common vertex. We obtain ρ^+ candidates by pairing π^0 candidates with an identified π^+. The ω candidates are reconstructed by combining a π^0 candidate with pairs of oppositely charged pion candidates that originate from a common vertex; the charged pion pair must be consistent with originating from the interaction region to suppress K^0_S decays. We select ρ (ω) candidates with an invariant mass satisfying $630 < m_{\pi\pi} < 940$ MeV/c^2 ($764 < m_{\pi^+\pi^-\pi^0} < 795$ MeV/c^2).

The high-energy photon from the signal B decay is identified as a neutral energy deposit in the calorimeter. We require that the deposit meet a number of criteria designed to eliminate background from charged particles and hadronic showers [10]. We veto photons from $\pi^0(\eta)$ decay by requiring that the invariant mass of the candidate combined with any other photon of laboratory energy greater than 30 (250) MeV not be within the range 105-155 MeV/c^2 (500-590 MeV/c^2).

The photon and ρ/ω candidates are combined to form the B-meson candidates. We define $\Delta E^* \equiv E^*_B - E^*_{\text{beam}}$, where E^*_B is the center-of-mass (c.m.) energy of the B-meson candidate and E^*_{beam} is the c.m. beam energy. The ΔE^* distribution of Monte Carlo (MC) simulated signal events is centered at zero, with a resolution of about 50 MeV. We also define the beam-energy-substituted mass $m_{\text{ES}} \equiv \sqrt{E^{*2}_{\text{beam}} - \text{p}^{*2}_B}$, where p^*_B is the c.m. momentum of the B candidate. Signal MC events peak in m_{ES} at the mass of the B meson m_B with a resolution of 3 MeV/c^2. The distribution of continuum and combinatorial $B\overline{B}$ background peaks in neither m_{ES} nor ΔE^*; the background distributions of $B \to K^*\gamma$, $B \to (\rho/\omega)\pi^0$, and $B \to (\rho/\omega)\eta$ peak at m_B in m_{ES} and between -190 MeV and -60 MeV in ΔE^*. We consider candidates in the ranges $-0.3 < \Delta E^* < 0.3$ GeV and $5.20 < m_{\text{ES}} < 5.29$ GeV/c^2 to incorporate sidebands that allow the combinatorial background yields to be extracted from a fit to the data.

Several variables that distinguish between signal and continuum events are combined in a neural network [11]. The input variables depend mainly on the rest of the event (ROE), defined to be all charged tracks and neutral energy deposits in the calorimeter not used to reconstruct the B candidate. To reject ISR events, we compute the ratio of second-to-zeroth order Fox-Wolfram moments [12] for the ROE and the ρ/ω candidate, in the frame recoiling against

the photon momentum. To discriminate between the jetlike continuum background and the more spherically symmetric signal events, we compute the angle between the photon and the thrust axis of the ROE in the c.m. frame and the moments $L_i \equiv \sum_j p_j^* \cdot |\cos\theta_j^*|^i / \sum_j p_j^*$, where p_j^* and θ_j^* are the momentum and angle with respect to an axis, respectively, for each particle j in the ROE. We use L_1, L_2, and L_3 with respect to the thrust axis of the ROE, as well as L_1 with respect to the photon direction. Differences in lepton and kaon production between background and B decays are exploited by including *BABAR* flavor tagging variables [13] as well as the maximum c.m. momentum and number of $K^\pm$ and K_S^0 in the ROE. For the $B^0 \to (\rho^0/\omega)\gamma$ modes, we also use the separation along the beam axis of the B-meson candidate and ROE vertices; to remove poorly reconstructed events we require the separation be less than 4 mm. A separate neural network is trained for each mode. We make a loose selection on the output of the neural network $\mathcal{N}$ that retains around 80% of the signal events.

To suppress background, we combine a number of signal-decay variables in a Fisher discriminant [14] $\mathcal{F}$ separately for each mode. We calculate the B-meson production angle θ_B^*, the ρ/ω helicity angle θ_H, which is defined with respect to the normal of the decay plane for ω candidates, and the ω Dalitz angle θ_D [7]. To reject $B \to \rho(\pi^0/\eta)$ and $B \to \omega(\pi^0/\eta)$ events in the $B^+ \to \rho^+\gamma$ and $B^0 \to \omega\gamma$ ($B^0 \to \rho^0\gamma$) selection, we require $|\cos\theta_H| < 0.70$ (0.75).

After applying the $\mathcal{N}$ and $|\cos\theta_H|$ criteria, the expected average candidate multiplicity in signal events is 1.15, 1.03, and 1.14 for $B^+ \to \rho^+\gamma$, $B^0 \to \rho^0\gamma$, and $B^0 \to \omega\gamma$, respectively; in events with multiple candidates the one with the smallest value of $|\Delta E^*|$ is retained.

The signal yield is determined from an extended maximum likelihood fit to the selected data. We fit the four-dimensional distribution of $m_{\rm ES}$, ΔE^*, $\mathcal{F}$, and $\mathcal{N}$. For the $B \to \rho\gamma$ fits, five event hypotheses are considered: signal, continuum background, combinatorial B background, peaking $B \to \rho(\pi^0/\eta)$ background, and peaking $B \to K^*\gamma$ background. For the $B^0 \to \omega\gamma$ fit we consider only signal, continuum background, and peaking $B \to \omega(\pi^0/\eta)$ background. The correlations among the observables are small; therefore, we assume that the probability density function (PDF) $\mathcal{P}(\vec{x}_j;\ \vec{\alpha}_i)$ for each hypothesis is the product of individual PDFs for the variables $\vec{x}_j = \{m_{\rm ES}, \Delta E^*, \mathcal{F}, \mathcal{N}\}$ given the set of parameters $\vec{\alpha}_i$. The likelihood function is a product over all N_k candidate events of the sum of the PDFs,

$$\mathcal{L}_k = \exp\Big(-\sum_{i=1}^{N_{\rm hyp}} n_i\Big)\Big\{\prod_{j=1}^{N_k}\Big[\sum_{i=1}^{N_{\rm hyp}} n_i \mathcal{P}_i(\vec{x}_j;\vec{\alpha}_i)\Big]\Big\},$$

where n_i is the yield of each hypothesis, k is the $B \to (\rho/\omega)\gamma$ mode, and $N_{\rm hyp} = 5(3)$ for $B \to \rho\gamma$ ($B \to \omega\gamma$).

The $m_{\rm ES}$ and ΔE^* PDFs are parametrized by a Crystal Ball function [15] for both the signal and peaking background. The parametrization is determined from signal MC samples, except the mean of the ΔE^* distribution, which is offset by the observed difference between data and MC samples of $B \to K^*\gamma$ decays. The continuum background $m_{\rm ES}$ and ΔE^* distributions are parametrized by an ARGUS threshold function [16] and a second-order polynomial, respectively. The combinatorial B background is described by a smoothed distribution [17] determined from MC events in both $m_{\rm ES}$ and ΔE^*. The distribution of $\mathcal{N}$ for signal and $B\overline{B}$ background is parametrized by a Crystal Ball function. The $\mathcal{N}$ distribution for continuum is determined from sideband data, and a histogram is used as the PDF. The distribution of $\mathcal{F}$ is parametrized by smoothed histograms of sideband data for the continuum background and MC events for all other hypotheses.

The fit to the data determines the shape parameters of the continuum background $m_{\rm ES}$ and ΔE^* PDFs, as well as the signal, continuum background, and combinatorial $B\overline{B}$ background yields. All other parameters are fixed, including the peaking $B\overline{B}$ background yields. A combined fit is also performed relating the modes using the definition of $\overline{\mathcal{B}}[B \to (\rho/\omega)\gamma]$ to determine an effective yield ($n_{\rm eff}$)

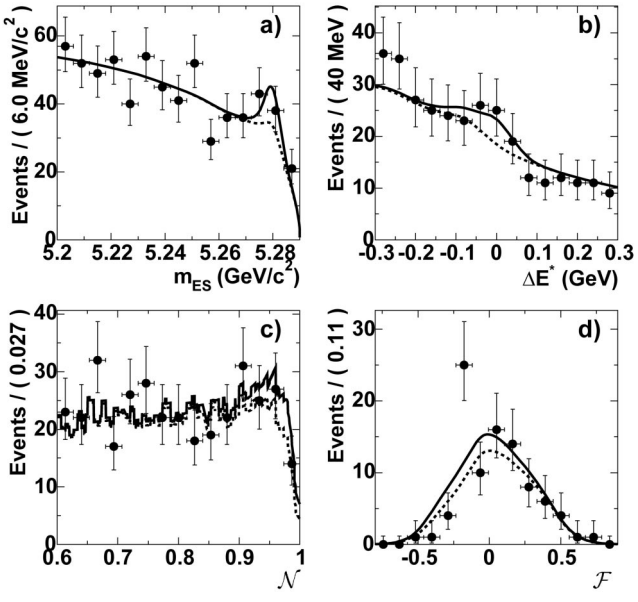

FIG. 1. Projections of the combined fit to $B \to \rho\gamma$ and $B^0 \to \omega\gamma$ in the four discriminating variables: (a) $m_{\rm ES}$, (b) ΔE^*, (c) $\mathcal{N}$, and (d) $\mathcal{F}$. The points are data, the solid line is the total PDF and the dashed line is the background only PDF. The selections applied, unless the variable is projected, are: $5.272 < m_{\rm ES} < 5.286$ GeV/c^2, $-0.10 < \Delta E^* < 0.05$ GeV, and $\mathcal{N} > 0.9$; the selection efficiencies for signal events are 45%, 57%, 70%, and 44% for the $m_{\rm ES}$, ΔE^*, $\mathcal{N}$, and $\mathcal{F}$ projections, respectively.

assuming $n[B^+ \to \rho^+\gamma] = n_{\rm eff} \cdot \epsilon[B^+ \to \rho^+\gamma]$ and $n[B^0 \to (\rho^0/\omega)\gamma] = \frac{1}{2}(\tau_{B^0}/\tau_{B^+}) n_{\rm eff} \cdot \epsilon[B^0 \to (\rho^0/\omega)\gamma]$, where n and ϵ are the yields and reconstruction efficiencies of each mode; the efficiencies include the daughter branching fractions. We take $\tau_{B^+}/\tau_{B^0} = 1.086 \pm 0.017$ [18]. Figure 1 shows the projections of the combined fit results compared to the data. The results for the individual mode signal yields and $n_{\rm eff}$ are given in Table I. The significance is computed as $\sqrt{2\Delta \log \mathcal{L}}$ where $\Delta \log \mathcal{L}$ is the log likelihood difference between the best fit and the null-signal hypothesis. No significant signal is observed.

The most important systematic uncertainties are associated with the modeling of $B\overline{B}$ backgrounds, the fixed parameters of the PDFs used in the fit, and the signal reconstruction efficiency. The first two contribute to the uncertainties on the signal yields.

The uncertainty on the peaking $B \to K^*\gamma$ background is dominated by the $K^\pm$misidentification rate; the rate is corrected by the difference in $K^\pm$ misidentification between data and MC samples of D^* decays, with the whole correction taken as the uncertainty. For the $B^+ \to \rho^+(\pi^0/\eta)$, $B^0 \to \rho^0\eta$, and $B^0 \to \omega(\pi^0/\eta)$ peaking background decays, we vary the branching fractions by either 1 standard deviation from the measured values or between zero and the measured upper limit if the decay has not been observed [19,20]; the value of the $B^0 \to \rho^0\pi^0$ branching fraction is varied between zero and 5.1×10^{-6} [20,21]. The uncertainty on the peaking background of each mode is shown in Table I. We find that the bias from neglecting the $B \to K^*\gamma$ background and combinatorial $B\overline{B}$ background in the fit to $B^0 \to \omega\gamma$ candidates is $1.1^{+1.9}_{-1.1}$ events; the corrected yield is given in Table I. To estimate the uncertainty related to the extraction of the signal $m_{\rm ES}$ and ΔE^* PDFs from MC distributions, we vary the parameters within their errors. The variation in the fitted signal yield is taken as a systematic uncertainty. The uncertainty related to the statistics of the histogram PDF that describes the continuum $\mathcal{N}$ distribution is evaluated by varying the binning and by using a fifth-order polynomial as an alternative PDF. Several different control samples of data and MC events were used to determine alternative PDFs for the different hypotheses; none of these resulted in a significant change to the fitted signal yield.

The signal efficiency systematic error contains uncertainties from tracking, particle identification, photon/π^0 reconstruction, photon selection, and the neural network selection that are determined as in Ref. [22]. We determine the effect of correlations among the fit variables by using an ensemble of MC experiments of parametrized continuum background simulations embedded in samples of fully simulated signal and $B\overline{B}$ background events. No bias is observed within the statistical error on the mean yields from this ensemble, which is taken as a multiplicative systematic uncertainty. The total multiplicative systematic error values are 11%, 13%, and 10% for $B^+ \to \rho^+\gamma$, $B^0 \to \rho^0\gamma$, and $B^0 \to \omega\gamma$, respectively. The corrected signal efficiencies and their uncertainties are shown in Table I.

In calculating branching fractions, we assume $\mathcal{B}(\Upsilon(4S) \to B^0\overline{B}^0) = \mathcal{B}(\Upsilon(4S) \to B^+B^-) = 0.5$. The 90% confidence level (C.L.) is taken as the largest value of the efficiency-corrected signal yield at which $2\Delta \log \mathcal{L} = 1.28^2$. We include systematic uncertainties by increasing the efficiency-corrected signal yield by 1.28 times its systematic uncertainty. Table I shows the resulting upper limits on the branching fractions.

Using the measured value of $\mathcal{B}(B \to K^*\gamma)$ [22], we calculate a limit of $\overline{\mathcal{B}}[B \to (\rho/\omega)\gamma]/\mathcal{B}(B \to K^*\gamma) < 0.029$ at 90% C.L. This limit is used to constrain the ratio of CKM elements $|V_{td}/V_{ts}|$ by means of the equation [3,6]:

$$\frac{\overline{\mathcal{B}}[B \to (\rho/\omega)\gamma]}{\mathcal{B}(B \to K^*\gamma)} = \left|\frac{V_{td}}{V_{ts}}\right|^2 \left(\frac{1 - m_\rho^2/M_B^2}{1 - m_{K^*}^2/M_B^2}\right)^3 \zeta^2[1 + \Delta R],$$

where ζ describes the flavor-SU(3) breaking between ρ/ω and K^*, and ΔR accounts for annihilation diagrams. Both ζ and ΔR must be taken from theory [3,6,23]. Following [3], we choose the values $\zeta = 0.85 \pm 0.10$ and $\Delta R = 0.10 \pm 0.10$, which is the average over the values given for the three modes. We find the limit $|V_{td}|/|V_{ts}| < 0.19$ at 90% C.L, ignoring the theoretical uncertainties. Our upper limit on $|V_{td}|/|V_{ts}|$ constrains $|V_{td}| < 0.008$ at 90% C.L. assuming $|V_{ts}| = |V_{cb}|$ [18]; this lies within the current 90% confidence interval $0.005 < |V_{td}| < 0.014$, which is obtained from a fit to experimental results on the CKM matrix elements [18]. Varying the values of ζ and ΔR within their

TABLE I. The signal yield ($n_{\rm sig}$), continuum background yield ($n_{\rm cont}$), peaking background ($n_{\rm peak}$), significance in standard deviations σ, efficiency (ϵ), and branching fraction ($\mathcal{B}$) central value and upper limit at the 90% C.L for each mode. The results of the combined fit are shown in the bottom row where $n_{\rm sig}$ is equal to $n_{\rm eff}$, which is described in the text. When two errors are quoted, the first is statistical and the second is systematic.

Mode	$n_{\rm sig}$	$n_{\rm cont}$	$n_{\rm peak}$	Significance (σ)	ϵ(%)	$\mathcal{B}(10^{-6})$	$\mathcal{B}(10^{-6})$ 90% CL
$B^+ \to \rho^+\gamma$	26^{+15+2}_{-14-2}	6850 ± 90	18 ± 4	1.9	13.2 ± 1.4	$0.9^{+0.6}_{-0.5} \pm 0.1$	<1.8
$B^0 \to \rho^0\gamma$	$0.3^{+7.2+1.7}_{-5.4-1.6}$	4269 ± 73	18 ± 7	0.0	15.8 ± 1.9	$0.0 \pm 0.2 \pm 0.1$	<0.4
$B^0 \to \omega\gamma$	$8.3^{+5.7+1.3}_{-4.5-1.9}$	1378 ± 37	$2.6^{+0.8}_{-1.2}$	1.5	8.6 ± 0.9	$0.5 \pm 0.3 \pm 0.1$	<1.0
Combined	$269^{+126+40}_{-120-45}$	—	—	2.1	—	$0.6 \pm 0.3 \pm 0.1$	<1.2

uncertainties leads to changes in the limits by ± 0.03 and ± 0.001 for $|V_{td}|/|V_{ts}|$ and $|V_{td}|$, respectively.

In conclusion, we have found no evidence for the exclusive $b \to d\gamma$ transitions $B \to \rho\gamma$ and $B^0 \to \omega\gamma$ in 211×10^6 $\Upsilon(4S) \to B\overline{B}$ decays studied with the *BABAR* detector. The 90% C.L. upper limits on the branching fractions and $|V_{td}|/|V_{ts}|$ are significantly lower than our previous values [7] and restrict the range indicated by SM predictions [3,4].

We are grateful for the excellent luminosity and machine conditions provided by our SLAC PEP-II colleagues, and for the substantial dedicated effort from the computing organizations that support *BABAR*. The collaborating institutions wish to thank SLAC for its support and kind hospitality. This work is supported by DOE and NSF (U.S.A), NSERC (Canada), IHEP (China), CEA and CNRS-IN2P3 (France), BMBF and DFG (Germany), INFN (Italy), FOM (The Netherlands), NFR (Norway), MIST (Russia), and PPARC (United Kingdom). Individuals have received support from CONACyT (Mexico), A. P. Sloan Foundation, Research Corporation, and Alexander von Humboldt Foundation.

*Present address: Department of Physics, University of Warwick, Coventry, United Kingdom
†Also at Università della Basilicata, Potenza, Italy.
‡Also at IFIC, Instituto de Física Corpuscular, CSIC-Universidad de Valencia, Valencia, Spain.
§Deceased.

[1] For a review, see K. Lingel, T. Skwarnicki, and J. G. Smith, Annu. Rev. Nucl. Part. Sci. **48**, 253 (1998).
[2] The named member of a charge-conjugate pair of particles stands for either.
[3] A. Ali, E. Lunghi, and A. Parkhomenko, Phys. Lett. B **595**, 323 (2004).
[4] S. W. Bosch and G. Buchalla, Nucl. Phys. **B621**, 459 (2002).
[5] See, for example, S. Bertolini, F. Borzumati, and A. Masiero, Nucl. Phys. **B294**, 321 (1987); H. Baer and M. Brhlik, Phys. Rev. D **55**, 3201 (1997); J. Hewett and J. Wells, Phys. Rev. D **55**, 5549 (1997); M. Carena *et al.*, Phys. Lett. B **499**, 141 (2001).
[6] A. Ali and A. Y. Parkhomenko, Eur. Phys. J. C **23**, 89 (2002).
[7] *BABAR* Collaboration, B. Aubert *et al.*, Phys. Rev. Lett. **92**, 111801 (2004).
[8] CLEO Collaboration, T. E. Coan *et al.*, Phys. Rev. Lett. **84**, 5283 (2000).
[9] *BABAR* Collaboration, B. Aubert *et al.*, Nucl. Instrum. Methods Phys. Res., Sect. A **479**, 1 (2002).
[10] *BABAR* Collaboration, B. Aubert *et al.*, Phys. Rev. Lett. **88**, 101805 (2002).
[11] We use the Stuttgart Neural Network Simulator (http://www-ra.informatik.uni-tuebingen.de/SNNS) to train a neural net with one hidden layer of five or six nodes.
[12] G. C. Fox and S. Wolfram, Nucl. Phys. **B149**, 413 (1979).
[13] *BABAR* Collaboration, B. Aubert *et al.*, Phys. Rev. Lett. **89**, 201802 (2002).
[14] R. A. Fisher, Annals Eugen. **7**, 179 (1936).
[15] E. D. Bloom and C. W. Peck, Annu. Rev. Nucl. Part. Sci. **33**, 143 (1983).
[16] ARGUS Collaboration, H. Albrecht *et al.*, Z. Phys. C **48**, 543 (1990).
[17] K. Cranmer, Comput. Phys. Commun. **136**, 198 (2001).
[18] Particle Data Group Collaboration, S. Eidelman *et al.*, Phys. Lett. B **592**, 1 (2004).
[19] *BABAR* Collaboration, B. Aubert *et al.*, Phys. Rev. Lett. **93**, 181806 (2004); Phys. Rev. D **70**, 032006 (2004).
[20] *BABAR* Collaboration, B. Aubert *et al.*, Phys. Rev. Lett. **93**, 051802 (2004).
[21] Belle Collaboration, J. Dragic *et al.*, Phys. Rev. Lett. **93**, 131802 (2004).
[22] *BABAR* Collaboration, B. Aubert *et al.*, hep-ex/0407003 [Phys. Rev. D (to be published)].
[23] B. Grinstein and D. Pirjol, Phys. Rev. D **62**, 093002 (2000).